Materials Horizons

Accepted Manuscript

ROYAL SOCIETY OF CHEMISTRY

rsc.li/materials-horizons

Conceptual Insight:

Hybrid materials combine multiple disparate components (e.g., organic/inorganic) at molecular or nanoscale level into one system. The hybridization endows these materials with desired properties that are otherwise often not available from each constituent. As a result, hybrid materials can find applications in diverse fields. Great efforts have been devoted to the development of new strategy for fabricating hybrid materials such as inorganic nanoparticle/hydrogel particles. The ability to manipulate the distribution of nanoparticles within hydrogels offers new opportunities to control the property of hybrid hydrogels. Particularly, the use of autonomous migration of nanoparticles for fabrication is conceptually novel and may advance the application of hybrid hydrogels.

Journal Name

RSCPublishing

COMMUNICATION

Formation of Hybrid Core-Shell Microgels Induced By Autonomous Unidirectional Migration of Nanoparticles

Cite this: DOI: 10.1039/x0xx00000x

Jianying Wang,[a,b,#] Kai Song,[b,c,#] Lei Wang,[b] Yijing Liu,[b] Ben Liu,[b] Jintao Zhu,[a] Xiaolin Xie,[a] and Zhihong Nie[b]

Received 00th January 2012,
Accepted 00th January 2012

DOI: 10.1039/x0xx00000x

www.rsc.org/

This Communication describes a facile strategy for the fabrication of inorganic nanoparticle (NP)-loaded hybrid core-shell microgels. The formation of core-shell microgels constitutes a novel mechanism in which the ionic-crosslinking of charged polymers (e.g., alginate) drives the unidirectional migration of NPs towards the centre of droplets. This versatile strategy allows the encapsulation of inorganic NPs with different sizes, shapes and surface properties in the core of the microgels in a single step.

Hybridization of microgels with inorganic nanoparticles (NPs) can endow the system with new or advanced functionalities that are often not attainable by any of individual components.[1-11] For instance, the integration of Au NPs in thermoresponsive microgels makes them responsive to light due to the photothermal effect of metal NPs (that is, the conversion of absorbed light to heat).[12] As a result of combined characteristic of organic and inorganic components, these hybrid microgels have been used as "smart" vehicles for the light triggered delivery of therapeutic agents.[6] When magnetic NPs are introduced, the hybrid microgels can be used as "smart" stabilizers for emulsions and the separation and stability of the emulsions can be manipulated by external magnetic field.[1] The optical, magnetic or catalytic properties of hybrid microgels are strongly dependent on the nature and spatial arrangement of NPs within the microgels. Among hybrid microgels with different morphologies, core-shell microgels are particularly attractive for applications in photonics, catalysis, sensing, and biomedicine, due to their unique characteristics, such as responsiveness to stimuli, superior biocompatibility, and tailorable physical property.[13-19]

Currently, hybrid core-shell microgels are usually fabricated by i) localized deposition of NPs within templates of core-shell emulsions or organic particles[20] and ii) coating as-synthesized inorganic NPs with polymers.[21] The former method involves the synthesis of organic core-shell particles, and the subsequent synthesis of inorganic NPs within the hydrogel reactor.[22-24] The latter approach relies on the coating of inorganic NPs with a hydrogel layer by various polymerization techniques (e.g., atom transfer radical polymerization).[25-27] These conventional approaches mostly utilize existing surfaces or interfaces between different materials to guide the formation of core-shell structures. However, they either require relatively sophisticated surface modification of NPs or can only be applied to limited types of inorganic NPs.

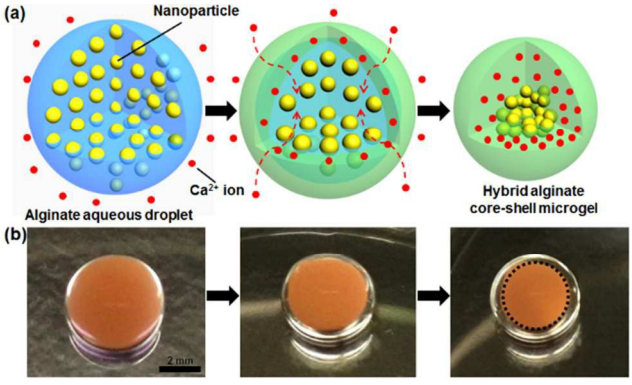

Figure 1. (a) Schematic illustration of the formation process of hybrid core-shell microgels via ionic crosslinking-induced migration of inorganic NPs. An aqueous alginate droplet containing NPs is immersed in a solution of CaI_2 in undecanol.

The continuous gelation of alginate by Ca^{2+} ions diffused into the droplet pushes the NPs radially into the center of the droplet (rather than locally trapping the NPs in the gel), leading to the formation of hybrid core-shell microgels. (b) Photographic demonstration of the formation of a hybrid core-shell microgel.

Herein, we report an unconventional strategy for the fabrication of hybrid core-shell microgels encapsulated with inorganic NPs within cores. This novel method utilizes the unexpected unidirectional migration of inorganic NPs radially towards the centre of an aqueous droplet of hydrogel precursors during the ionic cross-linking of charged polymers (e.g., sodium alginate) by metal ions (e.g., Ca^{2+}) (Figure 1). The shell thickness and core size of the hybrid particles can be controlled by tuning the concentration of NPs ([NP]) or Ca^{2+} ions ($[Ca^{2+}]$). This facile approach does not require laborious surface modification of NPs, as in most conventional methods. This method is applicable to the fabrication of hybrid core-shell microgels from different combination of hydrogels (e.g., alginate, carrageenan, and carboxymethyl cellulose) and inorganic NPs, such as Au NPs, Au nanorods (NRs), silica NPs, Fe_3O_4 magnetic NPs, CdSe quantum dots (QDs) (see Figure S1 in SI). The use of NPs with different surfaces, sizes, shapes, and compositions dictates the unique features and resulting applications of such hybrid core-shell microgels.

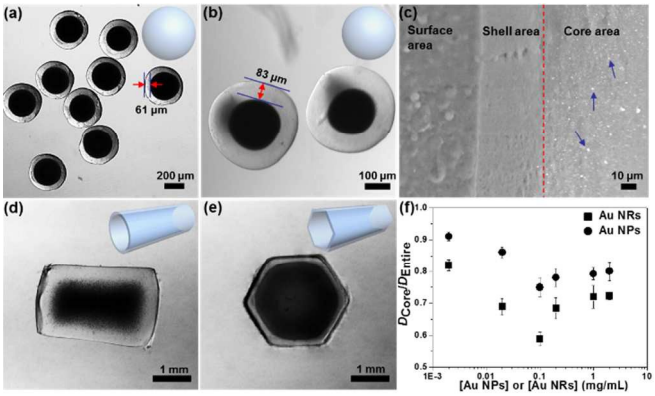

Figure 2. (a, b) Optical image of spherical hybrid alginate core-shell microgels with Au NRs concentrated in cores. The concentration of NRs in the initial droplets is 1.0 mg/mL (a) and 0.1 mg/mL (b). (c) SEM image of the cross-section of a hybrid core-shell microgel with concentrated Au NPs as cores. Bright dots (indicated by blue arrows) are NPs encapsulated in the core. (d, e) Optical image of non-spherical hybrid core-shell microgels with cylindrical shape (d) and hexagonal prism-like shape (e). Insets indicate the shape of tubes used as templates for confining alginate droplets. (f) Dependence of D_{Core}/D_{Entire} on the concentration of Au NPs or NRs.

Results and discussion

We used a microfluidic technique to generate monodispersed water-in-oil emulsion droplets (see experimental details in SI).[28-31] An aqueous solution containing sodium alginate, inorganic NPs (e.g., Au NRs), and poly(vinyl alcohol) (PVA) surfactant was used as the droplet phase, while undecanol was used as the continuous phase. When the two liquids were forced through a narrow orifice, monodispersed droplets were generated in the downstream channel (Figure S2). The droplets were collected in a solution of CaI_2 (~ 0.1-2 wt %) in undecanol. The Ca^{2+} ions in undecanol slowly diffused into alginate droplets and gradually crosslinked sodium alginate.[32] The crosslinking of polymer chains propagated radially from the interface towards the centre of the droplets. It is surprising that the ionic crosslinking of alginate triggered the unidirectional migration of NPs to form a core with concentrated NPs (Figure 1b). This phenomenon differs from our intuition that gelation traps the NPs locally within the corsslinked polymer networks to produce microgels with uniform distribution of NPs. After the complete solidification, the microgels shrunk by ~10-50% in diameter, depending on the crosslinking density of the biopolymer.

Figure 2a,b shows representative hybrid core-shell alginate microgels with Au NRs (~ 95 nm in length and ~ 30 nm in diameter) as cores. The presence of Au NRs in the centre area of microgels provides high contrast between the core and shell phases. The shell thickness of the core-shell microgels can be tailored by controlling the concentration of NRs. Using the same method, spherical Au NPs can be loaded in the core of microgels. The accumulation of NPs in the core was confirmed by imaging the cross-section of a fractured hydrogel particle using scanning electron microscope (SEM) (Figure 2c). A sharp interface between the core and shell phase can be clearly observed: the majority of NPs are presented in the core, while almost no NPs can be found in the shell region. This approach allows us to readily prepare hybrid core-shell hydrogel particles with controlled shapes (e.g., cylinder-like and hexagonal prism-like microgels) by confining the droplets within a shape-defined geometry (Figure 2d,e) (see experimental details in SI).

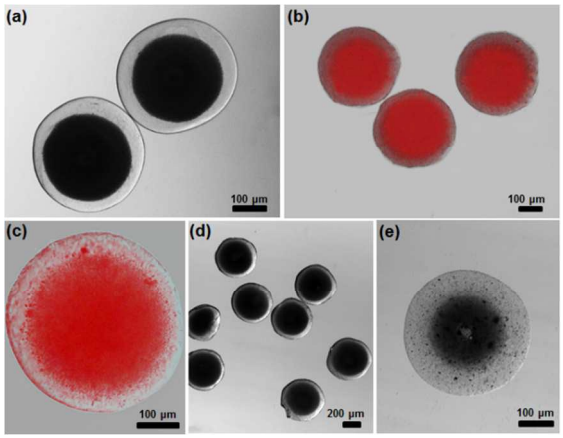

Figure 3. (a) Optical image of hybrid core-shell microgels with Au NPs in the cores. (b, c) Merged images from optical and fluorescence images of hybrid core-shell microgels with Rhodamin B doped silica NPs (b) and QDs (c) in the cores. (d, e) Optical images of hybrid core-shell microgels with $CaCO_3$ NPs (d) and Fe_3O_4 NPs (e) in the cores.

The overall diameter of the hybrid core-shell particles can be tuned in the range of 10-900 μm by varying the size of the alginate droplets (Figure S3a, b). The core size of the hybrid microgels can be controlled by varying [Ca^{2+}] or [NP]. When [Ca^{2+}] was increased from 0.1 to 2.0 wt % and other parameters were kept as constant, the ratio of core size to overall size of hybrid microgels (D_{Core}/D_{Entire}) first decreased from ~ 0.75 to 0.6 and then increased from ~ 0.6 to 0.8 (Figure S3c). This can be explained by the delicate interplay of the driving force for NP migration arising from ionic crosslinking and the friction to slow down the migration of NPs due to the crosslinked polymer networks. On one hand, the fast ionic crosslinking occurred at high [Ca^{2+}] provides strong forces to accelerate the unidirectional movement of NPs.[33] On the other hand, the formation of dense polymer networks resulting from fast crosslinking hinders the migration of NPs. Similar trend was also observed when [NP] was increased. The D_{Core}/D_{Entire} first decreased from ~ 0.9 to 0.75 and then increased from ~ 0.75 to 0.8, when [NP] was increased from 0.001 to 2 mg/mL (Figure 2f).

This general approach is applicable to the generation of core-shell microgels from NPs with different sizes, shapes, compositions, and surface properties (Figure 3). Firstly, we demonstrated that NPs with size ranging from ~ 3 to 350 nm can be encapsulated in the core of microgels in a single step (see images of NPs in Figure S1). They include such as QDs (~ 3-5 nm), Fe_3O_4 NPs (~ 10-15 nm), Au NPs (~ 30 nm), $CaCO_3$ NPs (~ 30-40 nm), and silica NPs (~ 350 nm) (Figure 3a-e). Secondly, NPs with different shapes (e.g., Au NRs and spherical NPs) can be encapsulated into the core of the microgels (Figure 2a and 3a). Thirdly, it is interesting that the encapsulation of NPs is not sensitive to the surface property of NPs. We demonstrate that all types of NPs can be integrated into alginate microgels as cores (Figure 2a and Figure 3), regardless of whether they are positively charged (e.g., Au NRs, $CaCO_3$ NPs, or Fe_3O_4 NPs), negatively charged (e.g., Au NPs, QDs), or neutral (e.g., silica NPs) (see Zeta potential measurements in Table S1 in SI). Moreover, other negatively charged biopolymers (e.g., I-carrageenan and sodium carboxymethylcellulose) can also be used for generating core-shell structures (Figure S4). The ability to integrate various NPs into core-shell microgels offers us a simple tool to tailor the multi-functionality of the particles (Figure S5). The hybrid microgels exhibit good stability in some organic solvents (e.g., ethanol) or acidic aqueous solution (e.g., pH=1) for weeks. However, when they are placed in an aqueous salt solution (NaCl at 100 mM), the hybrid microgels slowly dissolved after about 24 hrs, due to the dissociation of ionic bonding between polymers at high ionic strength.[34]

To understand the formation mechanism of hybrid microgels with core-shell structures, we studied the kinetics of the shell-forming process (Figure S6). The propagating front of the gel was carefully measured as a function of time (t). Figure 4a summarizes the advancing rate of the gel front ($v_{Advancing}$) for three cases: i) pure biopolymer system in the absence of NPs; ii) system with the presence of positively charged Au NRs; and iii) system with the presence of negatively charged Au NPs. We observed that the propagating front of crosslinked gels was consistent with the back of the migration line of NP swarms, when NPs were used. Moreover, our control experiment showed that slow UV-initiated polymerization of droplets containing N-isopropyl acrylamide, N,N'-methylene-bis-acrylamide and initiator (Irgacure 2959) did not cause the unidirectional migration of NPs to produce hybrid core-shell microgels (Figure S7 and S8). Together these results suggest that the ionic crosslinking of biopolymers drives the unidirectional movement of NPs towards the centre of the droplet to form cores.

Numerically, $v_{Advancing}$ can be derived based on the diffusion and reaction stoichiometry.[35] The flux of alginate (J_a) and flux of Ca^{2+} (J_c) consumed by the reaction zone in the vicinity of the gel front are given by:

$$J_c = -D_c \cdot \frac{\partial C}{\partial x} \quad (1)$$

$$J_a = v_{Advancing} \cdot A_o \quad (2)$$

Where D_c is the diffusion coefficient of Ca^{2+} ions through alginate gel, C is the concentration of Ca^{2+} ions at x position, and A_o is the initial concentration of bulk sodium alginate. In the traveling wave approximation, stoichiometrically equivalent amount of alginate must be converted to gel by the Ca^{2+} reaching the reaction zone, given by:

$$J_c = -N_c \cdot J_a \quad (3)$$

Where N_c is the the stoichiometric coefficient of the Ca^{2+}—alginate reaction. Therefore, we can derive:

$$D_c \cdot \frac{\partial C}{\partial x} = N_c \cdot v_{Advancing} \cdot A_o \quad (4)$$

The solving of the boundary conditions of the eq (4) yields the expression for $v_{Advancing}$ as:

$$v_{Advancing} = \frac{1}{2}\left(\frac{2D_c \cdot C_o}{N_c \cdot A_o \cdot t}\right)^{1/2} \quad (5)$$

Where C_o is the initial concentration of Ca^{2+} ions in undecanol.

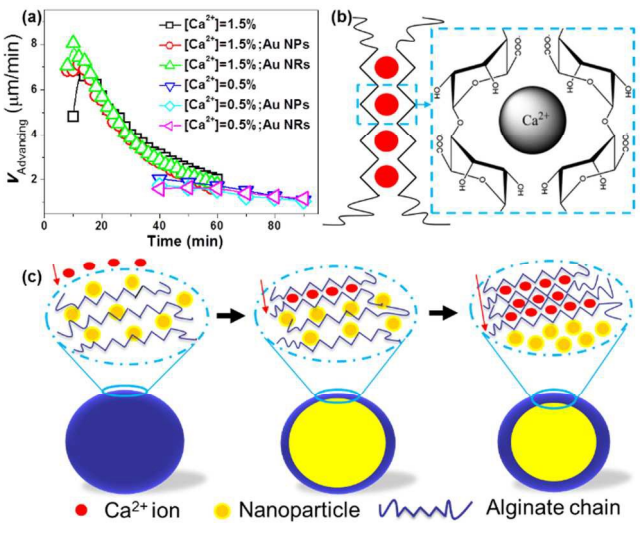

Figure 4. (a) The evolution of $v_{Advacing}$ as a function of time with and without the addition of NPs in the alginate droplets. (b)

Schematic illustration of the formation of an "egg-box", arising from the coordination between a single Ca^{2+} cation and four sugar units from two polymer chains. (c) Schematic illustration of the proposed formation mechanism of hybrid core-shell microgels based on an "egg-box" model. Red arrows indicate the diffusion direction of Ca^{2+} ions.

First of all, the $v_{Advancing}$ exponentially decays as a function of reaction time from eq. (5) due to the reduced diffusion rate of Ca^{2+} through crosslinked alginate gels, which is in good agreement with experimental measurements (Figure 4a). Secondly, both numerical and experimental results indicate that the $v_{Advancing}$ increased with the increase in the initial concentration of Ca^{2+} ions (C_o) (Figure 4a). More importantly, we observed that the presence of NPs, and the size and surface property of NPs do not affect the $v_{Advancing}$. The $v_{Advancing}$ of positively or negatively charged NPs are almost consistent with that of pure biopolymer system at various concentrations of Ca^{2+} ions. This result ruled out the possible diffusiophoresis mechanism in which a charged colloidal particle undergoes diffusiophoretic migration under the electric field arising from the flux of charged ions.[36] We are aware that the possible absorption of negatively charged sodium alginate on both positively charged and neutral NPs may alternate the charges on NPs. It is noted that the overall charge of droplets are negative, regardless of the charges carried by NPs (SI Table S2, S3).

In the light of current "egg-box" model ─ coordination between a single Ca^{2+} cation and four sugar units from two neighboring polymer chains (Figure 4b) ─ for ionic crosslinking of hydrogels,[37-40] we propose a possible mechanism for the formation of core-shell hydrogel structures through the unidirectional migration of NPs (Figure 4c). Upon the gradual diffusion of Ca^{2+} ions into the droplets, alginate chains first form "egg-box" structures and further produce nanofibrils with a diameter of ~ 10-15 nm. The long axis of the nanofibrils is perpendicular to the diffusion direction of Ca^{2+} flux. The formation of fibrils and their orientation has been previously confirmed in different ionic-crosslinked hydrogel systems (e.g., alginate, carrageenan, carboxymethylcellulose, and chitosan) by small-angle X-ray scattering.[41] The "zipping" of polymer chains to form "egg-box" structures and nanofibrils pushes NPs to migrate along the direction of Ca^{2+} flux, that is, the centre of droplets. However, the exact interactions underlying this process are still not clear, and further investigation is needed in future work.

Conclusions

In summary, we have demonstrated an unconventional approach for the preparation of hybrid core-shell hydrogel particles with different shapes and morphologies. The unidirectional NP immigration induced by ionic-crosslinking of polymers distinguishes our technique from any existing approaches. This method we developed shows at least three advantages over conventional techniques: i) It is simple and robust, and does not require any sophisticated surface modification of NPs; ii) It can be applied to the fabrication of hybrid core-shell microgels from different combinations of inorganic NPs and ionic polymers; and iii) It offers excellent control over the overall size, shell thickness, shape, and composition of hybrid microgels. The unique capability offered by this work will potentially advance the application of hybrid core-shell microgels in diverse areas, such as photonics, sensing, biomedicine, catalysts, and micro-motor (Figure S9).

Acknowledgements

Z.N. acknowledges the support of NSF Career Award (DMR-1255377) and startup funds from University of Maryland. J.Z. gratefully acknowledges funding provided by MOST (973 program, 2012CB821500), NSFC (51525302, 51173056 and 91127046). We also acknowledge the support of Maryland NanoCenter and its NispLab. The NispLab is supported in part by the NSF as a MRSEC Shared Experimental Facilities.

Notes and references

[a] Key Laboratory for Large-Format Battery Materials and System of the Ministry of Education, School of Chemistry and Chemical Engineering, Huazhong University of Science and Technology, Wuhan, 430074, China
E-mail: jtzhu@mail.hust.edu.cn

[b] Department of Chemistry and Biochemistry, University of Maryland, College Park, Maryland 20742, United States
E-mail: znie@umd.edu

[c] School of Life science, Changchun Normal University, Changchun 130031, China

[#] These authors contribute equally to this work.

† Footnotes should appear here. These might include comments relevant to but not central to the matter under discussion, limited experimental and spectral data, and crystallographic data.
Electronic Supplementary Information (ESI) available: [details of any supplementary information available should be included here]. See DOI: 10.1039/c000000x/

[1] M. Das, H. Zhang, E. Kumacheva, *Annu. Rev. Mater. Res.* **2006**, *36*, 117.
[2] L. A. Lyon, A. Fernandez-Nieves, *Ann. Rev. Phys. Chem.* **2012**, *63*, 25.
[3] M. Karg, T. Hellweg, *Curr. Opin. Colloid Interface Sci.* **2009**, *14*, 438
[4] M. Karg, *Colloid. Polym. Sci.* **2012**, *290*, 673.
[5] J. Pérez-Juste, I. Pastoriza-Santos, L. M. Liz-Marzán, *J. Mater. Chem. A* **2013**, *1*, 20.
[6] M. Das, L. Mordoukhovski, E. Kumacheva, *Adv. Mater.* **2008**, *20*, 2371.
[7] Z. X. Guo, M. Zhang, L. B. Zhao, S. S. Guo, X. Z. Zhao, *Biomicrofluidics* **2011**, *5*, 026502.
[8] C. H. Yeh, Q. Zhao, S. J. Lee, Y. C. Lin, *Sens. Actuators, A* **2009**, *151*, 231.
[9] J. M. Köhler, A. März, J. Popp, A. Knauer, I. Kraus, J. Faerber, C. Serra, *Anal. Chem.* **2013**, *85*, 313.

[10] J. W. Kim, A. S. Utada, A. Fernández-Nieves, Z. B. Hu, D. A. Weitz, *Angew. Chem. Int. Ed*. **2007**, *46*, 1819.
[11] Y. J. Zhao, H. C. Shum, H. S. Chen, L. L. A. Adams, Z. Z. Gu, D. A. Weitz, *J. Am. Chem. Soc.* **2011**, *133*, 8790.
[12] B. M. Budhlall, M. Marquez, O. D. Velev, *Langmuir* **2008**, *24*, 11959-11966.
[13] W. T. Wu, T. Zhou, A. Berliner, P. Banerjee, S. Q. Zhou, *Chem. Mater.* **2010**, *22*, 1966.
[14] D. Suzuki, H. Kawaguchi, *Langmuir* **2006**, *22*, 3818.
[15] Y. Lu, S. Proch, M. Schrinner, M. Drechsler, R. Kempeb, M. Ballauff, *J. Mater. Chem.* **2009**, *19*, 3955-3961.
[16] S. Shi, L. Zhang, T. Wang, Q. Wang, Y. Gao, N. Wang, *Soft Matter* **2013**, *9*, 10966.
[17] R. A. Álvarez-Puebla, R. Contreras-Cáceres, I. Pastoriza-Santos, J. Pérez-Juste, L. M. Liz-Marzán, *Angew. Chem., Int. Ed.* **2008**, *48*, 138.
[18] W. T. Wu, S. Q. Zhou, *Nano Rev.* **2010**, *1*, 5730.
[19] A. K. Gaharwar, N. A. Peppas, A. Khademhosseini, *Biotechnol. Bioeng*. **2014**, *111*, 441.
[20] J. Zhang, S. Xu, E. Kumacheva, *J. Am. Chem. Soc.* **2004**, *126*, 7908.
[21] R. Contreras-Cáceres, A. Sánchez-Iglesias, M. Karg, I. Pastoriza-Santos, J. Pérez-Juste, J. Pacifico, T. Hellweg, A. Fernández-Barbero, L. M. Liz-Marzán, *Adv. Mater.* **2008**, *20*, 1666.
[22] D. Suzuki, H. Kawaguchi, *Colloid Polym. Sci*. **2006**, *284*, 1443.
[23] B. Kim, H. Lee, J. Kim, S. H. Kim, *Chem. Commun*. **2013**, *49*, 1865.
[24] W. C. Jeong, S. H. Kim, S. M. Yang, *ACS Appl. Mater. Interfaces* **2014**, *6*, 826.
[25] M. Karg, T. Hellweg, *J. Mater. Chem.* **2009**, *19*, 8714.
[26] D. J. Kim, S. M. Kang, B. Kong, W. J. Kim, H. J. Paik, H. Choi, I. S. Choi, *Macromol. Chem. Phys.* **2005**, *206*, 1941.
[27] M. Karg, S. Jaber, T. Hellweg, P. Mulvaney, *Langmuir* **2011**, *27*, 820.
[28] J. T. Zhu, R. C. Hayward, *Angew. Chem., Int. Ed.* **2008**, *47*, 2113.
[29] H. Zhang, E. Tumarkin, R. Peerani, Z. H. Nie, R. M. A. Sullan, G. C. Walker, E. Kumacheva, *J. Am. Chem. Soc.* **2006**, *128*, 12205.
[30] E. Tumarkin, E. Kumacheva, *Chem. Soc. Rev.* **2009**, *8*, 2161.
[31] H. Zhang, E. Tumarkin, R. M. A. Sullan, G. C.Walker, E. Kumacheva, *Macromol. Rapid Comm.* **2007**, *28*, 527.
[32] J. Y. Sun, X. Zhao, W. R. K. Illeperuma, O. Chaudhuri, K. H. Oh, D. J. Mooney, J. J. Vlassak, Z. G. Suo, *Nature* **2012**, *489*, 133.
[33] M. Golmohamadi, K. J. Wilkinson, *Carbohydr. Polym.* **2013**, *94*, 82.
[34] S. K. Bajpai, S. Sharma, *React. Funct. Polym*. **2004**, 59 129.
[35] T. Braschler, A. Valero, L. Colella, K. Pataky, J. Brugger, P. Renaud, *Anal. Chem.* **2011**, *83*, 2234.
[36] B. Abécassis, C. Cottin-Bizonne, C. Ybert, A. Ajdari, L. Bocquet, *Nat. Mater.* **2008**, *7*, 785.
[37] G. T. Grant, E. R. Morris, D. A. Rees, P. J. C. Smith, D. Thom, *FEBS Lett.* **1973**, *32*, 195.
[38] E. R. Morris, D. A. Rees, D. Thom, J. Boyd, *Carbohydr. Res.* **1978**, *66*, 145.
[39] L. B. Li, Y. P. Fang, R. Vreeker, I. Appelqvist, *Biomacromolecules* **2007**, *8*, 464.
[40] P. Sikorski, F. Mo, G. Skjåk-Bræk, B. T. Stokke, *Biomacromolecules* **2007**, *8*, 2098.
[41] Y. Maki, K. Ito, N. Hosoya, C. Yoneyama, K. Furusawa, T. Yamamoto, T. Dobashi, Y. Sugimoto, K. Wakabayashi, *Biomacromolecules* **2011**, *12*, 2145.

TOC Graphic:

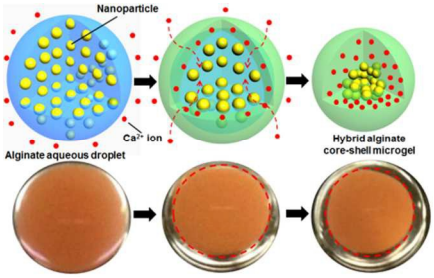

Abstract: A facile and unconventional strategy has been developed for the fabrication of inorganic nanoparticles (NPs)-loaded hybrid core-shell microgels. The formation of core-shell microgels constitutes a novel mechanism in which the ionic crosslinking of charged polymers (e.g., alginate) drives the unidirectional migration of NPs towards the center of droplets.